Smart Agricultural Technology 6 (2023) 100325

Contents lists available at ScienceDirect

Smart Agricultural Technology

journal homepage: www.journals.elsevier.com/smart-agricultural-technology

Remote sensing hail damage on maize crops in smallholder farms using data acquired by remotely piloted aircraft system

Mbulisi Sibanda [a,*], Helen S Ndlovu [b], Kiara Brewer [c], Siphiwokuhle Buthelezi [b], Trylee N Matongera [b], Onisimo Mutanga [b], John Odindi [b], Alistair D Clulow [c], Vimbayi G P Chimonyo [d,e], Tafadzwanashe Mabhaudhi [d,f]

[a] Department of Geography, Environmental Studies & Tourism, Faculty of Arts, University of the Western Cape, Private Bag X17, Robert Sobukwe Road, Bellville, South Africa
[b] The University of KwaZulu-Natal, Discipline of Geography and Environmental Science, School of Agricultural Earth and Environmental Sciences, Private Bag X01, Scottsville, Pietermaritzburg 3209, South Africa
[c] Discipline of Agrometeorology, School of Agricultural, Earth and Environmental Sciences, University of KwaZulu-Natal, Private Bag X01, Scottsville, Pietermaritzburg 3209, South Africa
[d] Centre for Transformative Agricultural and Food Systems, School of Agricultural, Earth and Environmental Sciences, University of KwaZulu-Natal (UKZN), Scottsville, Pietermaritzburg 3209, South Africa
[e] International Maize and Wheat Improvement Center (CIMMYT)-Zimbabwe, Mt Pleasant, Harare P.O. Box MP 163, Harare, Zimbabwe
[f] International Water Management Institute (IWMI), Pretoria 0184, South Africa

ARTICLE INFO

Edited by Stephen Symons

Keywords:
Hail damage
Small-scale croplands
UAVs
Remote sensing
Random forest

ABSTRACT

Smallholder farmers reside in marginal environments typified by dryland maize-based farming systems. Despite the significant contribution of smallholder farmers to food production, they are vulnerable to extreme weather events such as hailstorms, floods and drought. Extreme weather events are expected to increase in frequency and intensity under climate change, threatening the sustainability of smallholder farming systems. Access to climate services and information, as well as digital advisories such as Robust spatially explicit monitoring techniques from remotely piloted aircraft systems (RPAS), could be instrumental in understanding the impact and extent of crop damage. It could assist in providing adequate response mechanisms suitable for bolstering crop productivity in a spatially explicit manner. This study, therefore, sought to evaluate the utility of drone-derived multispectral data in estimating crop productivity elements (Equivalent water thickness (EWT), Chlorophyll content, and leaf area index (LAI)) in maize smallholder croplands based on the random forest regression algorithm. A hailstorm occurred in the study area during the reproductive stages 2 to 3 and 3 to 4. EWT, Chlorophyll content, and LAI were measured before and after the storm. Results of this study showed that EWT, Chlorophyll content, and LAI could be optimally estimated based on the red edge and its spectral derivatives. Specifically, EWT was estimated to a rRMEs 2.7% and 59%, RMSEs of 5.31 gm^{-2} and 27.35 gm^{-2}, R^2 of 0.88 and 0.77, while chlorophyll exhibited rRMSE of 28% and 25%, RMSEs of 87.4 μmol m^{-2} and 76.2 μmol m^{-2} and R^2 of 0.89 and 0.80 and LAI yielded a rRMSE of 10.9% and 15.2%, RMSEs of 0.6 m^2/m^2 and 0.19 m^2/m^2 before and after the hail damage, respectively. Overall, the study underscores the potential of RPAS-based remote sensing as a valuable resource for assessing crop damage and responding to the impact of hailstorms on crop productivity in smallholder croplands. This offers a means to enhance agricultural resilience and adaptability under climate change.

Introduction

Natural disasters such as hail storms, droughts and floods are now frequent and impact negatively on the livelihoods of smallholder farmers, especially their food and nutrition security [11]. Hailstorms, in particular, are expected to change in frequency due to variations in climate warming. While there is global uncertainty regarding the consequences of anthropogenic climate change on the frequency of severe weather phenomena such as hailstorms and associated economic losses, works by Rädler et al., [43] and Havenga [26] suggest an increase in the

* Corresponding author.
E-mail address: msibanda@uwc.ac.za (M. Sibanda).

https://doi.org/10.1016/j.atech.2023.100325
Received 21 June 2023; Received in revised form 14 September 2023; Accepted 15 September 2023
Available online 20 September 2023

frequency of hailstorm occurrences in Africa. Literature estimates that the annual damage caused by hailstorms will increase by between 25 and 50% [44,47]. These severe calamities often result in the loss of livestock and human life, agricultural equipment, crops, and soils, disrupting the growing season and production [11]. Meanwhile, smallholder farmers, especially in developing regions, are more susceptible to natural disasters because they rely on natural resources with limited finances. Hence their agriculture system is a low input/yield, making it difficult to attain food and nutrition security. Specifically, 70% of the population in Sub-Saharan Africa relies on agriculture for their livelihood, 50% of them are smallholder farmers and a portion of the 1.2 billion live on less than a dollar a day [7]. Smallholder farmers dominate the food production sector in many developing countries occupying about 30% of the agricultural lands, generating half of the food calories globally and about 70% of calories [48]. According to Kamara et al. [31] 80% of the food consumed in Sub-Saharan Africa is produced by smallholder farmers at a subsistence level. However, underdevelopment, lack of policies incorporating smallholder farmers, reliance on unpredictable precipitation, severe degradation of soils, an increase in the population and natural disasters are exacerbating the food demands while diminishing the chances of achieving food and nutrition security.

Maize is the most critical staple food crop covering 25 million ha in Sub-Saharan Africa, overwhelming impacting people livelihoods [52, 57]. Specifically, maize provides 50% half of the calories and protein consumed by Eastern and Southern Africans and 85 kg/capita/year of maize is consumed in Southern Africa [52]. The consumption of maize is over 100 kg/capita/year in Malawi, Lesotho, Zambia, Zimbabwe and South Africa [52]. This explains why it's a popular crop in smallholder croplands.

The overreliance on maize in several countries is a cause for concern regarding food and nutrition security is concerned in light of the changing climate. Natural disasters such as hailstorms have been instrumental in reducting maize yields, especially in smallholder croplands. Subsequently, there is an urgent need to develop and establish site-specific technologies for providing spatial explicit information on crop health that is suitable for informed and sound decision-making processes to optimize the production of maize.

Remote sensing is the most suitable technology that could offer spatially explicit information required in making informed and sound decisions in maize farm operations and in assessing the spatial extent of natural disasters such as hailstorms [41]. Remote sensing technologies offer a platform for systematically monitoring maize production spatially explicitly. However, the engagement of remote sensing technologies in forecasting maize crop production in Africa is at an infant stage [12,60]. The limited research efforts utilized low to medium-resolution remotely sensed data in mapping and monitoring crop attributes especially in Africa [19]. Low and medium spatial resolution remotely sensed data tends to mask out critical information required to discriminate and characterize various attributes of a specific crop such as maize in a heterogenous and highly fragmented cropland area. Using freely available data from missions such as Landsat and Sentinel becomes challenging in African smallholder croplands [9,40].

The advancements in earth observation facilities have brought about a new frontier, remotely piloted aircraft systems (RPAS), often called 'drones', for mapping and monitoring crop attributes across the growing season in small heterogenous croplands. The auspiciousness of RPASs in smallholder maize crop monitoring stems from their being innovative, relatively low cost, deploy at user-defined times as well as, offering ultrahigh spatial resolution near-real time spatial data which is effective for circumventing the challenges associated with low and medium resolution satellite-borne remotely sensed data [9,12,60].

RPAS-acquired remotely sensed data have been effectively used in mapping different maize crop attributes in various regions including southern Africa [9,13,40,60,66]. For instance, Wahab et al., [60] utilized RPAS-acquired remotely sensed data (NDVI) to estimate maize health and yield. Their results demonstrated that RPAS-derived Green Normalized Difference Vegetation Index (GNDVI) is an optimal proxy of crop health and a better estimator of yields with $r = 0.372$ and $r = 0.393$ for mean and maximum GNDVI respectively, at about five weeks after planting. Meanwhile, Chivasa et al., [13] explored using RPAS remotely sensed data characterising the maize varietal response to maize streak virus (MSV) disease. Their findings showed that manual MSV scores correlated highly with RPAS-acquired data (R^2 = 0.74–0.84). They classified maize into MSV-resistant, moderately resistant, and susceptible classes to an overall classification accuracy of 77.3% and a Kappa of 0.64. The work of Ndlovu et al., [40] and Brewer et al., [9] optimally estimated maize crop chlorophyll content and various foliar moisture elements (R^2 = 70–90). Despite the high accuracies associated with the RPAS-acquired data sets in assessing crop attributes, to the best of our knowledge, there are no studies that have sought to assess the utility of RPAS remotely sensed data in evaluating the impact of natural disasters such as hailstorms, especially at a field scale. Therefore, there is a need to extend research efforts towards identifying as well as assessing the optimal crop attributes for characterizing the spatial extent and magnitude of damage resulting from disasters such as hailstorms.

Besides the influence of ultrahigh spatial resolution data, the literature indicates that the engagement of robust and efficient machine learning algorithms improves the estimation of plant attributes in agroecological remote sensing applications. Specifically, algorithms such as the random forest (RF) ensemble have been tried and tested across different agro-ecological remote sensing applications. Yet, they emerged as the most robust, efficient and accurate [3,16]. Although no machine learning algorithm is suitable for a specific application, RF has become popular because i) it reduces overfitting through its bootstrap mechanism, ii) does not require normalizing of data, iii) selects optimal prediction input features, iv) it less sensitive to the sample sizes and it can adequately deal with complex relationships between auto-correlated descriptors [15]. In this regard, RF was perceived to be the most optimal algorithm suitable for detecting and assessing the impact of the hailstorm on maize crop parameters as a proxy for characterizing the spatial extent and magnitude of the hailstorm. Specifically, this study sought to evaluate the utility of drone-derived multispectral data in estimating crop productivity elements (Equivalent water thickness (EWT), Chlorophyll content, and leaf area index (LAI)) in maize smallholder croplands based on the random forest regression algorithm before and after the hailstorm as proxies for spatially quantifying the spatial extend and magnitude of the hailstorm in smallholder croplands.

Methods and materials

Study area

This study was conducted in Swayimane, a communal rural area within uMshwathi local municipality in KwaZulu Natal, South Africa (29°31′ 24'' S; 30° 41′37'' E) (Fig. 1). Smallholder subsistence crop farming systems dominate the land use in this area. Specifically, maize, sweet potatoes and taro (amadumbe) are the most dominant crops cultivated in these smallholder croplands. In farming these crops, smallholder farmers practice traditional farming techniques in planting maintaining and harvesting. For instance, manure derived from livestock is used as fertilizer, while ploughing and weeding are conducted manually in these farms. Smallholder farming is a form of food and nutrition security and a livelihood. Maize was planted in 3 plots measuring approximately 15 m x 50 m on 8 February 2021 and harvested on 26 May 2021 across a growth cycle of 108 days. Specifically, the phenological growth stage of maize crops considered in the study was between the day of the year 41 and day of the year (DOY) 147. The elevation at the experimental plots ranged from 839 to 850 m amsl [9, 40]. Crop farming in Swayimane is supported by a climate characterized by warm, wet summers and cool, dry winters. Swayimani receives a mean annual rainfall between 600 mm and 1200 mm and an average annual temperature of 24 °C [9,40]. Most of the precipitation in

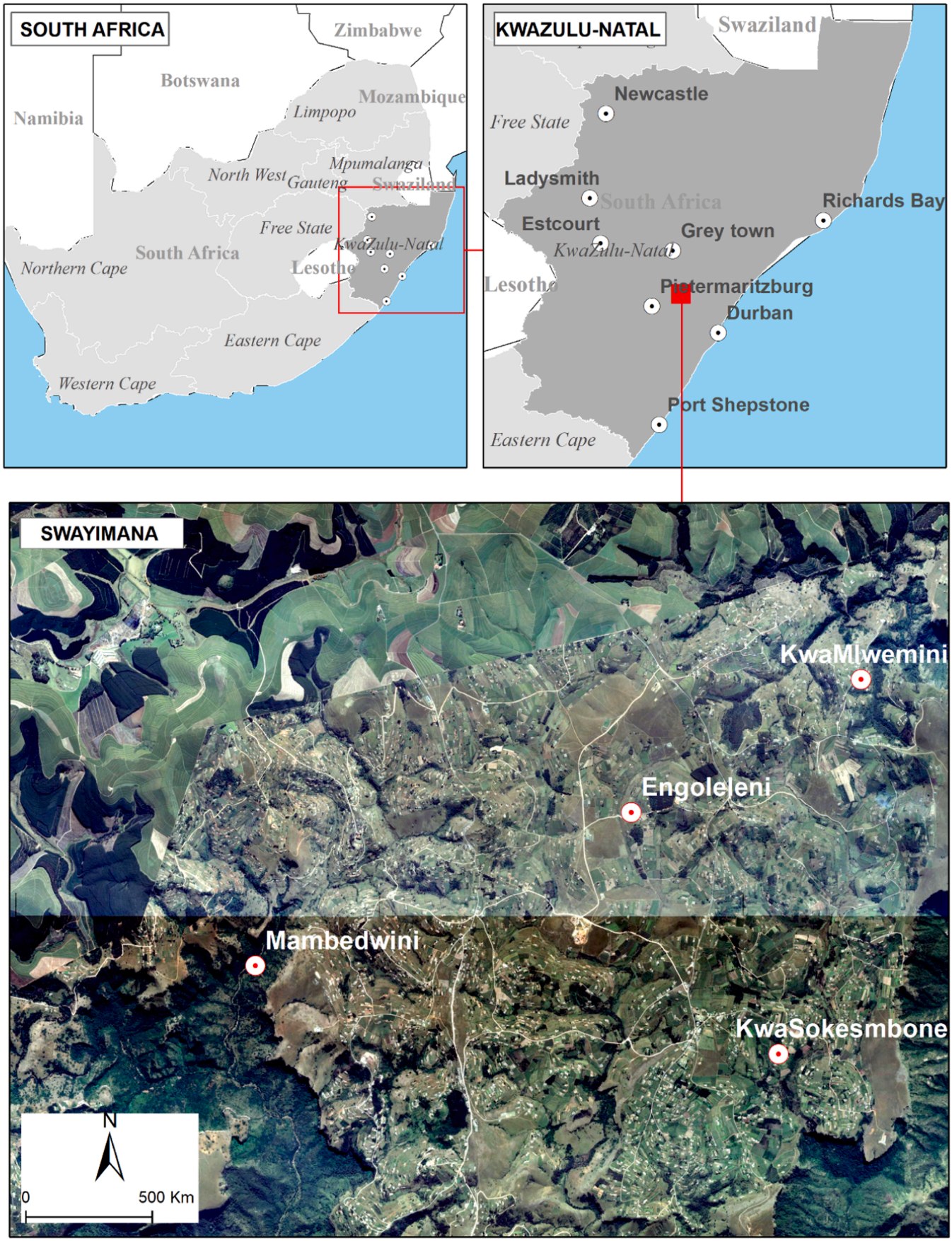

Fig. 1. Swayimane communal Area, in Umshwathi District, KwaZulu Natal Province, South Africa.

Swayimane occurs in summer, associated with thunder and hailstorms. Hailstorms are one of the primary disasters that generally decrease production in this area. In this regard, a hailstorm occurred on DOY 144 between maize's early and mid-reproductive(Fig. 2).

Field sampling

We generated sampling points across the experimental field plot before any measurement of leaf area index, chlorophyll content and equivalent water thickness. A polygon was digitized around the experimental plot and saved as a keyhole markup language file (kml). The kml file was then used to generate random sampling points where crop data was to be derived. It was also used to generate the flight plan to acquire the images. The kml was first imported into ArcMap 10.5, and 63 sample points were generated. These points were then imported into a handheld Trimble Global Positioning System (GPS) with sub-meter accuracy. These were then used as waypoints for navigation to the sampling point, where maize crop parameters were measured before and after the storm. The maize plants that coincided with the location of the sampling point were marked and considered in this experiment. If the point did not coincide with a plant, a plant within proximity was considered in this experiment. Then, maize crop leaf area index, chlorophyll content and equivalent water thickness were measured every two weeks across the growing season. This research was opportunistic and conducted after a hailstorm occurred during an experimental study [9,40].

To measure chlorophyll content, a Konica Minolta soil plant analysis development (SPAD) 502 chlorophyll meter (Minolta Corporation, Ltd., Osaka, Japan) was employed to measure chlorophyll content unitless values which were then converted into leaf chlorophyll content. The SPAD method of quantifying chlorophyll is desired and preferred in the community of practice because of the instrument's portability, and the noninvasiveness of the procedure followed to acquire the measurements. SPAD unitless values were converted to chlorophyll content in micromoles per square meter (μmol m^{-2}) following the universal model derived by Markwell et al.,'s [35] with $R^2 = 0.94$ detailed below:

$$Chl\ (\mu \mathrm{mol\ m^{-2}}) = 110^{s^{0.0265}}$$

Chl is the total chlorophyll per unit leaf area in μmol/m^{-2} and the *S* is the unitless SPAD value. The SPAD meter readings were conducted on one leaf per plant. Specifically, the newest fully expanded leaf with an exposed collar and a minimum width > 7 cm was considered to measure chlorophyll. These specific leaves were chosen because they were above the canopy, directly interacting with the incident radiation generating the crop's spectral signature used in this study. Readings were acquired at the midpoint of each leaf blade close to the vein, about 1 and 2/3 away from the leaf tip to avoid the leaf edge effects. The three readings were averaged and recorded from each sampling point. 63 chlorophyll measurements were recorded.

A hand-held Li-Cor LAI 2200 plant canopy analyzer was used to measure leaf area index estimates. The LAI estimate measurements were conducted under fairly clear conditions as explained in the instrument's user support guide (https://www.licor.com/env/support/LAI-2200C/topics/sky-conditions.html) (See Fig. 2). A half-open cap was used to avoid external influences and in consideration of the variability of maize plants as explained in the instrument's brochure (https://www.licor.com/env/pdf/area_meters/LAI-2200_brochure.pdf). In measuring each LAI estimate, five readings were conducted above and below the canopy of the maize plants. Initially, a reading was conducted above the canopy and then four other readings were conducted below the canopy. The Li-Cor LAI 2200 compares the above and below readings of radiation transmittances following an inversion of the Poisson model. The measurements below the canopy were conducted at about 30 cm above the ground to avoid weeds and foliage after the hailstorm. 63 LAI estimates were recorded.

In measuring the canopy equivalent water thickness of maize first fully developed leaf (first leaf below whorl) was acquired from the plants at each sampling point. Then a portable LI-3000C area meter with an LI-3050C (Li-Cor, USA) transparent belt Conveyer with a millimeter resolution was used to measure the leaf area (A). The leaf's fresh weight (FW) was then measured using a calibrated digital scale with a 0.5 g measurement error. The samples were then stored in brown paper bags, labelled according and taken to the laboratory where they were oven-dried at 70 until a constant dry weight (DW) was reached. Subsequently, the FW and DW were then utilized to drive EWT using the following formula;

$$\mathrm{EWT_{leaf}(gm-2)} = (\mathrm{FW-DW})/\mathrm{A}.$$

63 EWT measurements were recorded. All field measurements were conducted between 1200 and 1400 Hrs to coincide with the image acquisition time. All data we combined in an Excel spreadsheet and converted into a point map in ArcGIS.

Image acquisition and processing

This study used a MicaSense Altum multispectral sensor mounted on a DJI Matrice 300 to remotely sense maize crops. The Altum multispectral sensor acquires remotely sensed data in the blue (475 nm), green (560 nm), red (668 nm), red-edge (717 nm), NIR (840 nm) and thermal (8000–14,000 nm). To acquire the image, the generated kml file of the field boundary was imported into the drone controller and used to

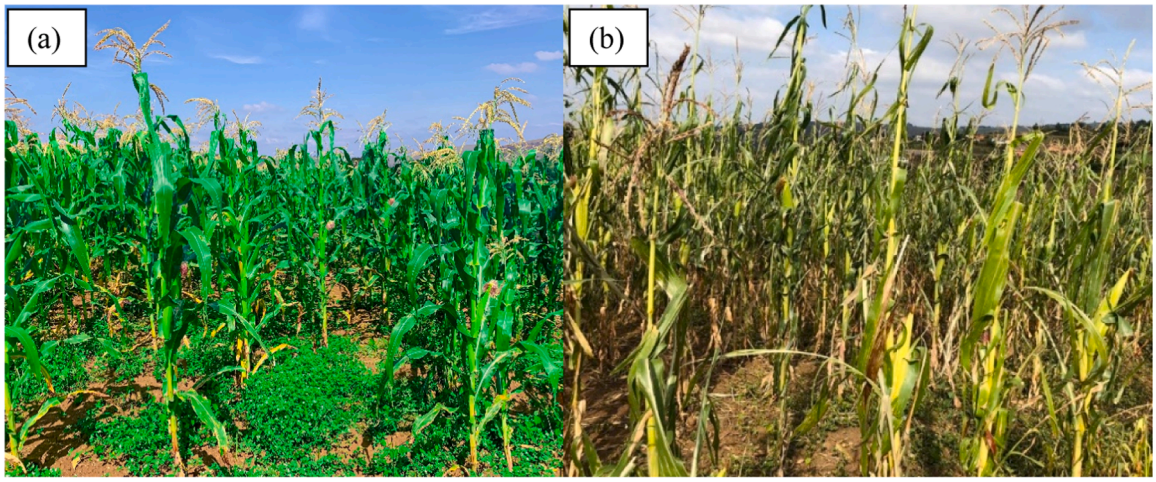

Fig. 2. State of maize crops (a) before the hailstorm during the early reproductive stage, and (b) after the hail storm during the mid-reproductive stage.

generate a flight path and conducting an automated flight. The acquired images had a resolution of 2064 × 1544 at 120 m (3.2 megapixels per multispectral band) and a ground sample distance (GSD) of 5.2 cm for the multispectral bands and 81 cm per pixel for the Thermal infrared at a height of 120 m.

Before and after the flights, a MicaSense Altum calibrated reflectance panel (CRP) was utilised to calibrate the sensor. The CRP is a white-balanced card that provides absolute reflectance values across the electromagnetic spectrum (EMS) wavelengths acquired by this sensor camera. To ascertain the stability of the aircraft during image acquisition, a predetermined route was generated using the flight controller, and the Waypoint Navigation flight mode was engaged. The autonomous Waypoint Navigation flight mode ensures the stability of the aircraft using a geofence which was a height of 120 m above the ground level (AGL). In addition to the intelligent internal GPS system of the DJI M300 system, a MicaSense DSL 2 sensor with an integrated GPS system was used to geotag the images, enhancing the geometric accuracy. 3576 images covering the study area were acquired and stitched per flight (before and after the hail storm). These images were then radiometrically corrected based on the CRP images using Pix4Dfields 1.8.0 (Pix4d Inc., San Francisco, CA, USA). The CRP reflectance is used by the Pix4Dfields software in radiometrically correcting the image. Pix4Dfields then generates a digital elevation model and the image based on the ground reference points acquired from the Google Earth Pro-domain. All images were projected, and the sampling points to the WGS 1984 UTM Zone 36S. Specifically, two images were acquired on DOY 102 before the hail storm and on DOY 118 after the hailstorm which occurred during DOY 114.

Maize reflectance data were then extracted from each band of the Pix4Dfields generated image following an overlay procedure using sampling point data in a GIS environment. The reflectance data were then used to compute vegetation indices for estimating the impact of the hailstorm on maize crop parameters (Table 1). These vegetation indices were selected based on their performance in the literature.

Statistical analysis

A random forest regression ensemble was used in this study to map EWT, LAI and Chlorophyll content. RF is an algorithm that stems from the family of decision trees ensembles which utilizes bootstrap aggregation and binary recursive partitioning to increase the number of independent trees [1]. The power of random forest is exhibited in its capability to utilize bootstrapping aggregation to grow regression trees to their maximal capacity and combine the results based on unweighted averaging to make predictions. This algorithm is popular because of its capacity to yield high accuracies while avoiding model overfitting issues. This is attained by searching for the optimal hyperparameter settings. These are the *Ntree,* the number of decision trees to be generated and *Mtry,* the number of predictor variables tested for the best split when growing the trees [5]. To identify the *Ntree* and *Mtry* values that can best predict maize that best estimated EWT, LAI and chlorophyll content before and after the hailstorm, the *Ntree* (the default value is 500 trees) values were tested from 500 to 9500, while *Mtry* was tested from 1 to 25 using a single interval [2,37].

Accuracy assessment

To assess the EWT, LAI and chlorophyll model accuracies the data were split into two datasets at a ratio of 70/30% for the training and testing datasets, respectively. In this regard, the root mean squared error (RMSE), relative root mean squared errorRRMSE%), and the coefficient of determination (R2) were computed and used to evaluate the

Table 1
Vegetation indices used in this study to estimate EWT, LAI and Chlorophyll content.

Vegetation Index	Abbreviation	Equation	
Normalized difference vegetation index	NDVI	$(NIR - RED)/(NIR + RED)$	[38,46,58]
Green normalized difference vegetation index	GNDVI	$\frac{NIR - GREEN}{NIR + GREEN}$	[38]
Red-green ratio index	RGR	$\frac{RED}{GREEN}$	[42]
Normalized difference red-edge index	NDRE	$\frac{NIR - RED\ EDGE}{NIR + RED\ EDGE}$	[4]
Corrected transformed vegetation index	CTVI	$\frac{NDVI + 0.5}{NDVI + 0.5} * (\sqrt{NDVI + 0.5})$	[39]
Infrared percentage vegetation index	IPVI	$\left(\frac{\frac{NIR}{NIR + RED}}{2}\right) * (NDVI + 1)$	[25]
Soil-adjusted vegetation index	SAVI	$\left(\frac{NIR - RED}{NIR + RED + L}\right) * (1 + L)$L is a constant between 0 and 1.	[28]
Optimized soil-adjusted vegetation index	OSAVI	$\frac{NIR - RED}{NIR + RED + 0.16}$	[45]
Green chlorophyll index	CI_{green}	$(NIR / GREEN) - 1$	[23]
Red-edge chlorophyll index	$CI_{rededge}$	$(NIR - RED\ EDGE) - 1$	[10]
Canopy chlorophyll content index	CCCI	$\frac{NIR - RED\ EDGE}{NIR + RED\ EDGE} / \frac{NIR - RED}{NIR + RED}$	[17]
Chlorophyll vegetation index	CVI	$NIR * \left(\frac{RED}{GREEN^2}\right)$	[59]
Modified chlorophyll absorption ratio index	MCARI	$\frac{1.5[2.5(NIR - RED) - 1.3(NIR - GREEN)]}{\sqrt{[(2NIR + 1)^2 - (6NIR - 5\sqrt{(RED)}) - 0.5}}$	[62]
Normalised Difference Water Index	NDWI	Green - NIR / Green + NIR	[20]
Red-Edge Normalised Difference Vegetation Index	$NDVI_{rededge}$	Rededge - Red / Rededge + red	[22]
Red-Blue Normalized Vegetation Index	BNDVI	$(NIR-(R + B))/(NIR+(R + B))$	[61]
Phenological Normalized Difference Vegetation Index	PNDVI	$(NIR-(G + R + B))/(NIR+(G + R + B))$	[8]
Simple Ration vegetation index	SR	NIR/R	[6]
Green Leaf Index	GLI	$((2*G)-R-B)/((2*G) + R + B)$	[34]
Enhanced Vegetation Index	EVI	2,5*((NIR-R)/(NIR+(6*R)-(7,5*B))+1)	[27]
Enhanced Vegetation Index 2	EVI3	$2,4*((NIR-R)/(NIR+R + 1))$	[36]
Enhanced Vegetation Index 3	EVI2	2,5*((NIR-R)/(NIR+(2,4*R)+1))	[30]
Modified normalised difference index	mNDVI	$(R_{Yi}) - (R_{Yj}) / (R_{Yi}) + (R_{Yj})$	[53]

Where RYi and RYj are any of the MicaSense Bands, i.e., Blue, Green, Red, Red Edge, NIR and Thermal bands.

magnitude of agreement between the predicted and field measured data as well as assessing the accuracy of the derived models.

Analysis stages

The first stage of this study was to select the spectral features that optimally estimated EWT, chlorophyll and LAI before and after the hailstorm, exclusively (Table 2). Bands and vegetation indices were used as input spectral features for estimating the LAI, chlorophyll and LAI. In the second stage, the most influential and frequent spectral features that optimally estimated EWT, chlorophyll and LAI were identified and chosen to be used to estimate the crop parameters. The selected spectral features had to be selected by random forest as an influential spectral feature (high VIP score) and appear in the analysis based on the image acquired before and after a storm. The same spectral features but computed using different images (i.e., the image acquired before and after the storm) were used to estimate EWT, chlorophyll and LAI in the second stage. In the final stage, the maps were created using the most optimal spectral features selected by RF in the second analysis stage.

Results

Descriptive statistics

This study showed that all crop parameters were relatively higher and drastically reduced by the hailstorm. For instance, Table 3 shows that the hailstorm reduced the mean of maize chlorophyll content from 6.51 μmol m^{-2} to 0.33 μmol m^{-2}. In comparison, EWT was reduced from 209.38 gm^{-2} to 96.48 gm^{-2}. Interestingly, LAI was increased by the hailstorm from an average of 3.29 m^2/m^2 to 5.15 m^2/m^2. All the data were assessed for normality using the Kolmogorov-Smirnov test, and all p-values were less than 0.05.

Predicting EWT, LAI and chlorophyll content before and after the hailstorm, using all features selected using RF

Before the hailstorm, EWT was estimated to have a RMSE of 5.31 gm^{-2} (rRMSE = 2.7%) and R^2 of 0.88 (Fig. 3(a)(i)) based on the NDVI, NIR NDWI, ClGreen, NDVIrededge, in order of importance (Fig. 4(a)(i)). A considerable decline in the estimation accuracies of maize EWT was observed after the hailstorm. Specifically, EWT was then estimated to a RMSE of 27.35 gm^{-2} (rRMSE = 59.1%) and R^2 of 0.65 (Fig. 3(a)(ii)) based on NDRE, NIR, NDWI, Clrededge, NDVI rededge and red edge in order of importance (Fig. 4(a)(ii)).

On the other hand, chlorophyll was optimally estimated before and after the hailstorm. Chlorophyll was estimated to have a RMSE of 76.2 μmol m^{-2} (rRMSE = 28%) and an R^2 of 0.75 (Fig. 3(b)(i)) based on the NDVI, NIR, Red edge, CLred edge, CCCI, NDRE (Fig. 4(b)(i)) in order of importance and amongst other variables. An optimal estimation was attained again after the hailstorm with a RMSE of 31.3 μmol m^{-2} and a R^2 of 0.78 (rRMSE =25%) (Fig. 3(b)(ii)) with the Red edge, NIR, MCARI, OSAVI, ENDVI, CTVI being the most influential spectral features (Fig. 4 (b)(ii)), in order of importance.

Table 2
Analysis stages followed in this study.

Analysis Stage	Description	Variables
1	Selections of optimal features for estimating EWT, chlorophyll content, and LAI for detecting the effect of the hail storm.	All bands and vegetation indices
2	Use of optimal spectral features derived in stage one to estimate crop parameters	Frequent influential spectral features in estimating each crop parameter before and after the storm.
3	Mapping the spatial distribution of crop parameters before and after the hailstorm	Optimal spectral features selected in Stage 2

Table 3
Descriptive statistics of EWT, LAI and Chlorophyll content before (DOY 118) and after (DOY 114) the hailstorm.

Crop Parameter	Day of year (DOY)	Growth stages	Minimum	Maximum	Mean
EWT (gm^{2})	102	R1 – R2	249.66	159.86	209.38
	118	R2 – R4	11.66	448.71	96.48
LAI (m^2/m^2)	102	R1 – R2	3.53	6.29	3.29
	118	R2 – R4	3.29	2.66	5.15
Chlorophyll (μmol m^{-2})	102	R1 – R2	104.2	3765.4	651.8
	118	R2 – R4	26.8	1555	33.1

LAI was also optimally estimated before and after the hailstorm. Before the storm, LAI was estimated to have a RMSE of 0.19 m^2/m^2 (rRMSE = 10.8%) and R^2 of 0.89 (Fig. 3(c)(i)) based on the modified nNDVI (NIR/Thermal), nNDVI (R/T), EVI2, GLI, nNDVI(R/Thermal), BNDIV as the most influential estimation spectral features (Fig. 4(c)(i)), in order of importance. After the storm, a RMSE of 0.32 m^2/m^2 (rRMSE = 15%) and R^2 of 0.91 (Fig. 3(c)(ii)) was obtained based on the nNDVI (NIR/B), nNDVI (G/NIR), nNDVI(Thermal/NIR/), RBNDVI as the most influential spectral variables (Fig. 4(c)(ii)), arranged in order of importance.

Predicting EWT, LAI and chlorophyll content before and after the hailstorm all features selected using RF

When optimal spectra features were used, EWT was estimated to have a RMSE of 25.88 gm^{-2} (rRMSE = 22%) and an R^2 of 0.80 before the storm (Fig. 5(a)(i)). In comparison, after the storm a RMSE of 27.98 gm^{-2} (rRMSE =24%) and a R^2 of 0.71 (Fig. 5(a)(ii)) were attained with the NDVIrededge, CCCI, CIgreen, NIR and nDVI (NIR/T) as the most influential spectral features, in order of importance (Fig. 5(a) (i&ii) Fig. 6(a)). Chlorophyll was estimated to have a RMSE of 70 μmol m^{-2} (rRMSE = 27%) and R^2 of 0.91, and a RMSE of 70 μmol m^{-2} (rRMSE = 29%) and R^2 of 92 were exhibited by NDRE, NDWI, Blue NDVrededge and CCCI as the most influential spectral features after the hailstorm, in order of importance (Fig. 5(b) (i&ii) Fig. 6(b)).

Meanwhile before the hailstorm, LAI was estimated to a RMSE of 0.26 m^2/m^2 (rRMSE = 16%) and R^2 of 0.72 and then a RMSE of 0.31 m^2/m^2 (rRMSE = 19%) and R^2 of 0.65 after the storm based on nDVI NIR/T nDVIT/B, nDVI G/R, CIrededge, nDVI B/NIR, GNDVI, BNDVI amongst among others, in order of importance (Fig. 5(c) (i&ii) Fig. 6(c)). Overall, it was observed that the red edge-based spectral features were the most frequent and influential in optimally mapping the effect of hailstorms on maize crop moisture and health parameters (Fig. 6(d)). The most optimal spectral variables were then used to estimate chlorophyl EWT, chlorophyll, and LAI before and after the hailstorm.

A significant variation was observed between the maps of maize crop parameters before and after the hailstorm (Fig. 7). All maps of maize crop parameters remotely sensed after the hailstorm are light in tone, showing reduced crop health and moisture content. For instance, before the storm, EWT was high at 450 (Fig. 7a), drastically reduced to about 285 by the hailstorm. Furthermore, it can be observed that the hailstorm mostly impacted maize crops in the western section of the fields while those in the eastern side were recovering quickly (Fig. 7).

Discussion

The study aimed to assess the prospects of utilizing RPAS-acquired remotely sensed data in estimating maize crop's EWT, chlorophyll content and LAI as proxies for assessing the effect of a hailstorm. Specifically, this study estimated maize crop EWT, chlorophyll content and

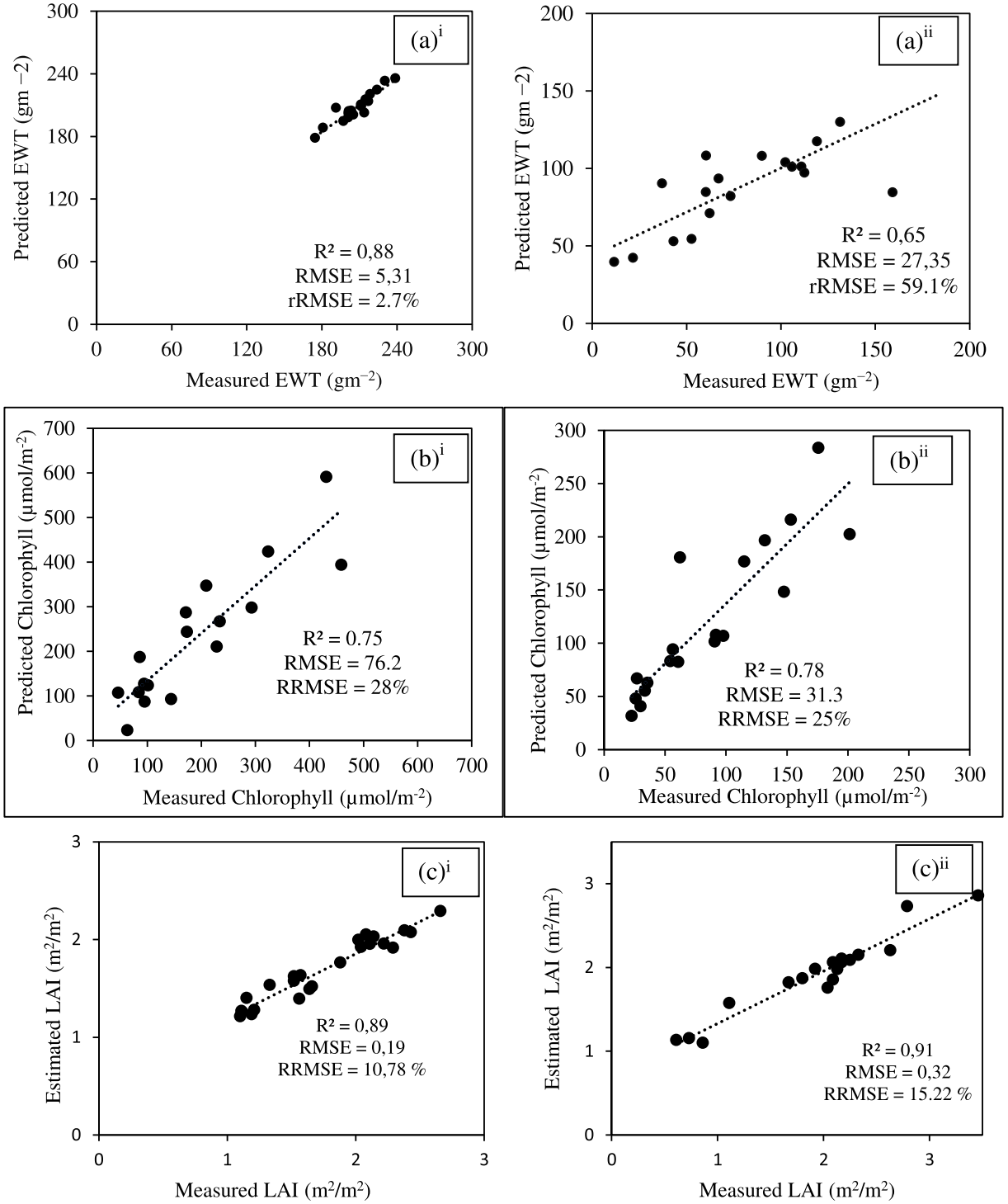

Fig. 3. Relationship between the RF predicted and estimated (a) EWT, (b) chlorophyll content and (c) LAI before (i) and after (ii) the storm.

LAI before and after the hailstorm using RF and RPAS-acquired spectral data and its derivatives in smallholder croplands.

Estimating maize crop EWT, chlorophyll content and LAI before and after the hailstorm using RF

The findings of this study showed that EWT could be optimally estimated before (RMSE = 25.88 gm^{-2}, R^2 = 0.80) and after (RMSE = 27.98 gm^{-2}, R^2 = 0.71) the hailstorm using NDVI red edge, CCCI, CIgreen, NIR and nDVI (NIR/T) as the most influential spectral features, in order of importance. The hailstorm generally destroys the leaves as shown in Fig. 2(b). The leaves often begin to wilt at the edges as they lose moisture. Specifically, the descriptive statistics indicated that the moisture content (mean EWT) decreased after the hailstorm. Meanwhile, when the plant is healthy, its cells will be turgid and full of moisture, highly photosynthesizing and producing more chlorophyll content. Subsequently, the chlorophyll content associated with high moisture content explains the optimal performance of red edge, NIR and thermal bands in estimating EWT. The red edge is the section on the EMS signature of plants where there is rapid inflection between the red and

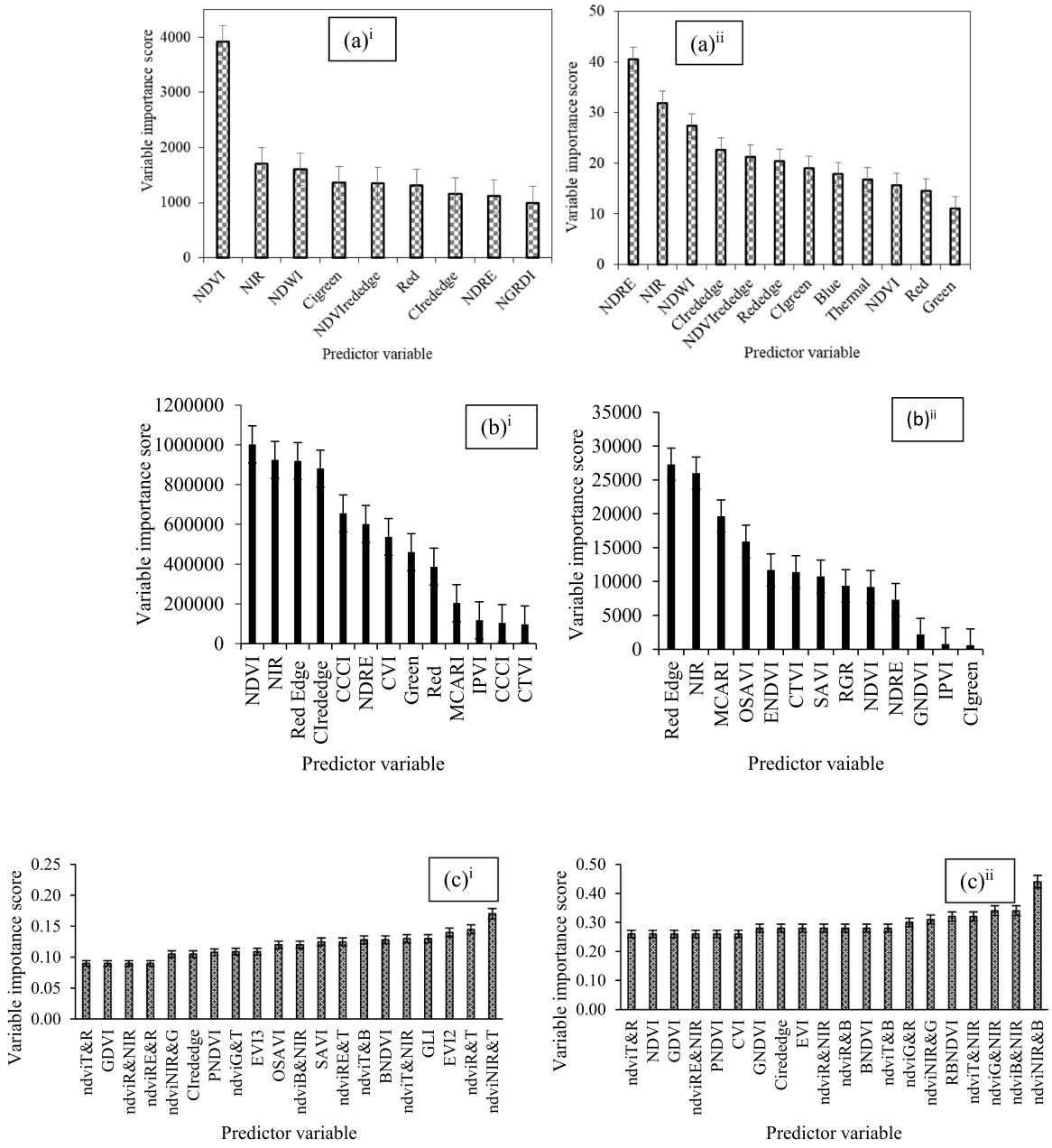

Fig. 4. Variable importance scores of features used in estimating (a) EWT, (b) chlorophyll content and (c) LAI before (i) and after (ii) the storm.

the NIR sections [18]. This section of the EMS is sensitive to the health of plants which generally are characterized by high moisture and chlorophyll content [18]. This section tends to shift towards the shortwave lengths when the plant is healthy. When hail hits the leaves, it compromises the plants' leaves and they begin to lose moisture and discolor as photosynthesis is altered. The alteration could be explained by a typical shift of the red edge section towards the longer wavelengths [18, 51,65]. These findings are similar to those of Zhang and Zhou [65], who also noted the red edge-based spectral variables were significantly sensitive to the maize crop's moisture canopy water content and EWT in their study on comparing crop water indicators in response to water stress treatments for summer maize in Hebei province, China. In a related study, YANG et al., [63] also reported that red edge-based vegetation indices were among the most influential independent variables that optimally modelled the LWC as a proxy for waterlogging stress on winter wheat using hyperspectral data in Yangzhou, China.

Results of the study also showed that NIR was another EMS that optimally estimated the effect of the hailstorm on maize crop EWT variation. A substantial and increasing amount of literature has proven that because of the water content in a healthy plant's leaves, NIR energy tends to be highly reflected providing the basis for remote sensing foliar moisture content [29,32,49,50,64] Literature notes that at the onset of moisture loss, typical of maize leaves after the hailstorm, there is a decrease in the reflectance of leaves, particularly in the NIR. Specifically, the epidermis to the mesophyll cells and air cavities in the leaf's facilitating the diffusion and scattering of the NIR radiation [32]. In contrast, the moisture content and the air spaces in the spongy mesophyll tend to be reduced due to dehydration, typical of the maize leaves after the storm, resulting in the absorption of the NIR radiation by leaves. Subsequently, the NIR section of the EMS becomes sensitive and instrumental in detecting the effect of hail damage on the maize crops.

Finally, the thermal section of the EMS was also noted to be influential in estimating the effect of hail on maize crop moisture content (EWT). This could be attributed to the fact that the thermal section of the

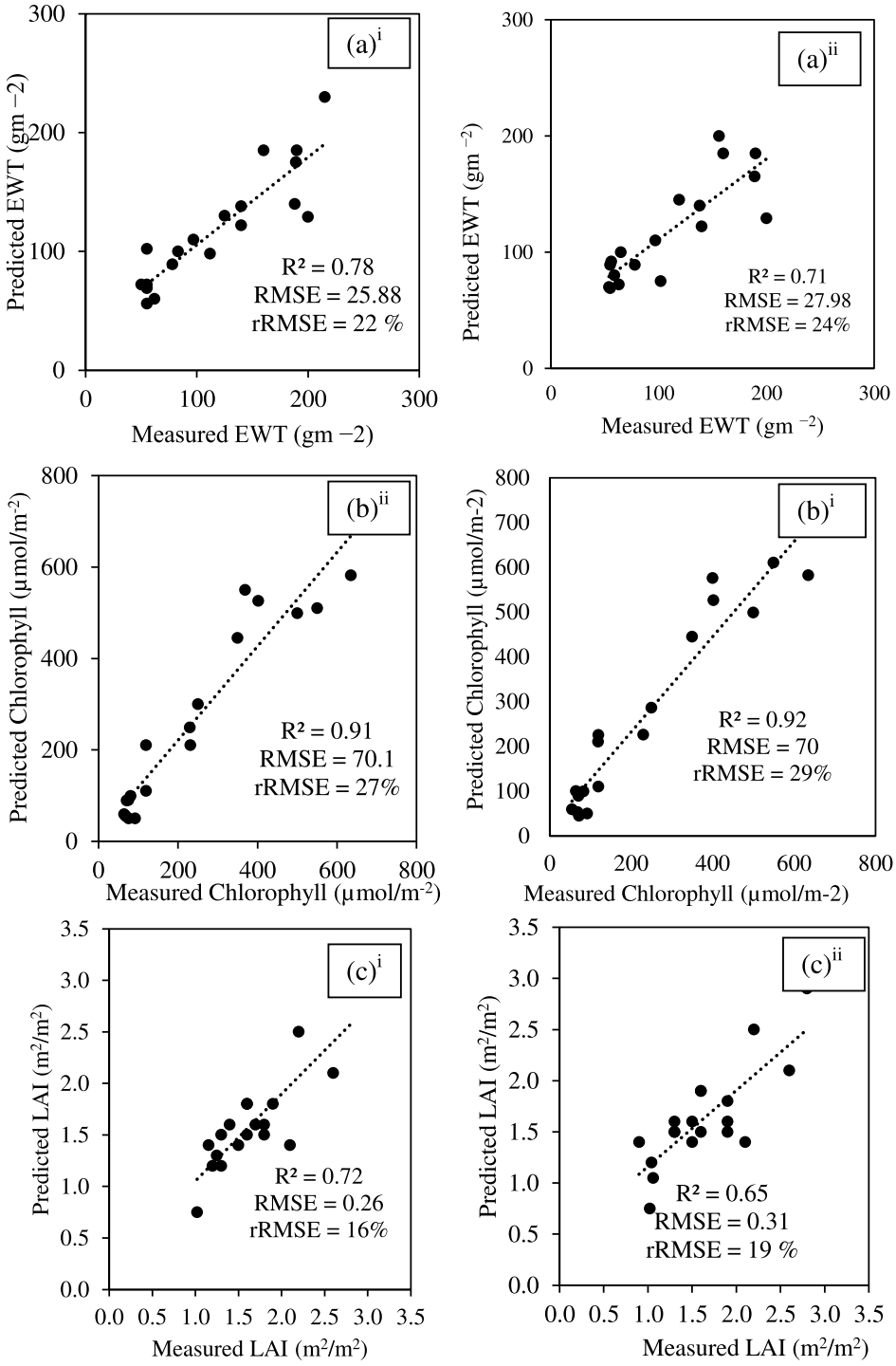

Fig. 5. Relationship between the RF predicted and estimated (a) EWT, (b) chlorophyll content and (c) LAI before (1) and after (2) the storm.

EMS tends to increase with the decrease in moisture content as the leaves wilt at the edge and discolor from the hail damage [21,33]. According to [21], when a plant incurs moisture stress, transpiration is reduced while foliar temperatures increase. This can then be detected by the thermal infrared section of the EMS as was the case in this study, where the thermal spectral features were selected, among others, as optimal variables for estimating the effect of hail damage on maize crop EWT.

Also, chlorophyll content was optimally estimated before (RMSE = 70 µmol m^{-2}, R^2 = 0.91) and after (RMSE =70 µmol m^{-2}, R^2 = 92) using NDRE, NDWI, Blue NDVrededge and CCCI as the most influential spectral features after the hailstorm, in order of importance. The influence of red edge can be attributed to a large and growing ample literature that attests to its sensitivity to chlorophyll content variations [9,14,54,56]. According to Curran et al., [14] there is a positive correlation between chlorophyll content and red edge reflectance. Before the hail, the maize crops are highly photosynthesizing, producing a lot of chlorophyll content, which is optimally detected by the red edge region of the EMA [23,24]. This maize crop's chlorophyll content is drastically reduced after the hailstorm as the plant attempts to heal from hail damage by senescing the torn sections of its leaves. As the senscence initiates, the chlorophyll content concentration is reduced, which is then

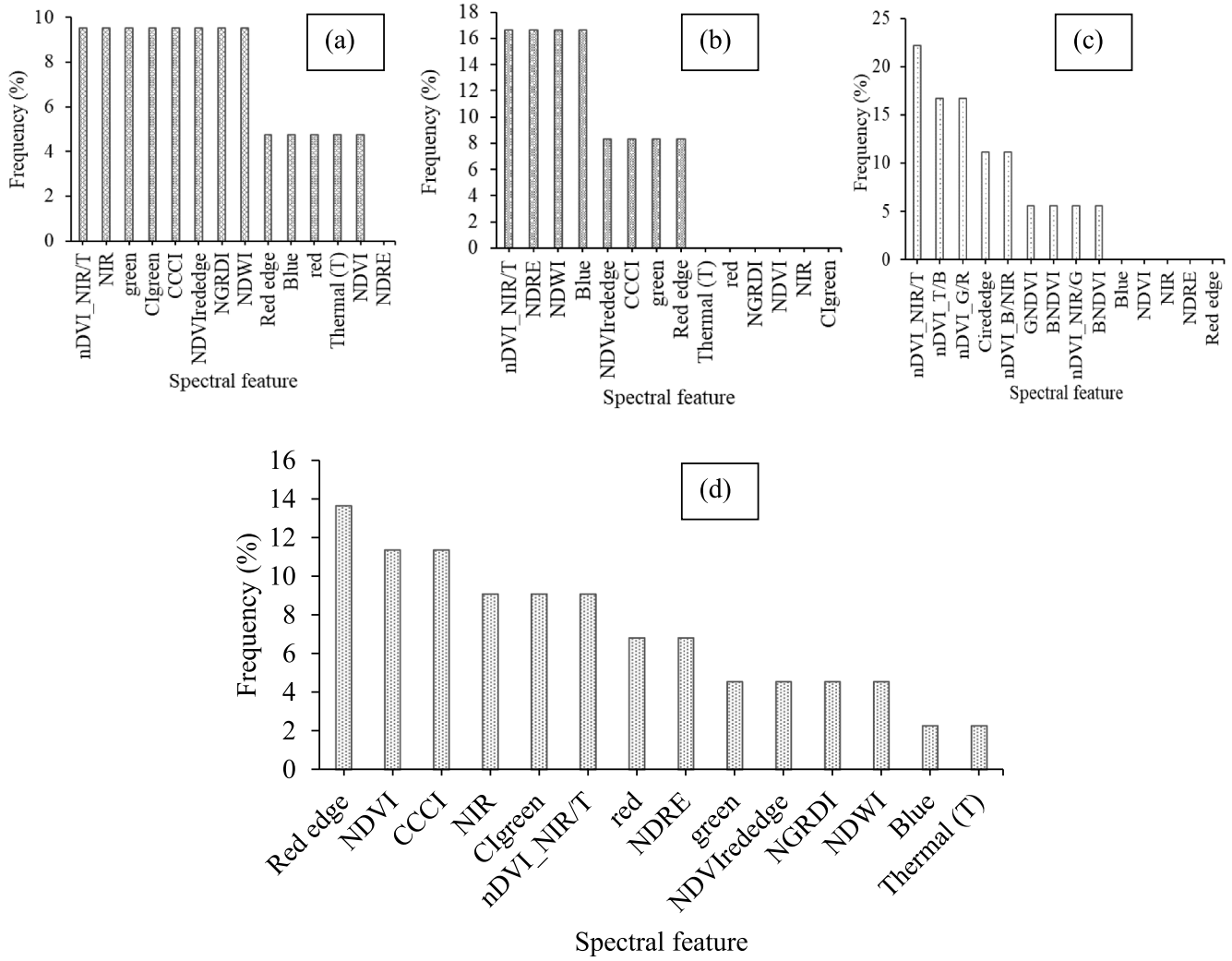

Fig. 6. Frequency of spectral features in optimally estimating the effect of the hailstorm on maize (a)EWT (b) chlorophyll (c) LAI and (d) across all parameters.

sensed by the red edge and its derivatives [55]. Meanwhile, NDWI is renowned for its sensitivity to plant moisture content variations; hence, it is not surprising that it was also among the optimal spectral features in estimating the effect of the hailstorm in this study.

Interestingly, the mean LAI increased after the hailstorm from 3.29 m^2/ m^2 to 5.15, respectively. This could be explained by an increase in the ground covered by leaves. After the hailstorm, some leaves on the plants hung downwards. Although these leaves may not have been optimally oriented for photosynthesis, they remained part of the canopy and were factored into the LAI measurements. The presence of these fresh leaves, bent downward but still connected to maize stems, could have effectively increased the leaf surface area, contributing to high LAI estimates. Before the hailstorm, maize leaves tended to be erect and turgid, facing the sky in competition for radiation, resulting in gaps in the canopy coverage.

The findings of this study also showed that LAI could be optimally estimated before (RMSE = 0.26 m^2/ m^2, $R^2 = 0.72$) and after (RMSE = 0.31 m^2/ m^2, $R^2 = 0.65$) using nDVI NIR/T nDVIT/B, nDVI G/R, CIrededge, nDVI B/NIR, GNDVI, BNDVI as the most optimal spectral features, in order of importance (Figs. 5(c)(i) and 6(c)(ii)). NDVI was the most frequent spectral feature in estimating LAI. This could be explained by a large and growing body of literature proving that the red, red edge, and NIR sections of the EMS are sensitive to the variations in the LAI. Specifically, an increase in the foliage is associated with an increase in photosynthetic activities which require red and blue radiation and an increase in the NIR reflectance due to the high moisture content in the palisade layer of the leaves. After the hailstorm, there is an increase in LAI estimate, but the plants are partly wilting with partially discoloured leaves. The blue radiation will no longer be absorbed but reflected. This triggers a reduction in the chlorophyll content and the green pigmentation, which could explain why the blue and the green bands based on modified nDVI were selected by RF as optimal estimation spectral features.

Despite the optimal influence of RPAS-acquired spectral features in estimating EWT, chlorophyll content and LAI, site factors such as topography could have exacerbated the spatial variation in the modelled maize crop health and productivity elements. The experimental site is characterized gradient which decreases from the east to the west. This was also noted in other studies conducted in the study area. In this regard, future studies should also consider the influence of situational factors generally exacerbated by natural disasters, negatively impacting crop productivity in smallholder croplands.

The implication of this study's findings

The findings imply that there are high prospects of employing RPASs in crop condition assessment at the field scale. In interpreting the findings of this study there is a need to consider that this study was conducted based on data acquired after a hailstorm and in only one field. Subsequently, there is a need for further studies to investigate the

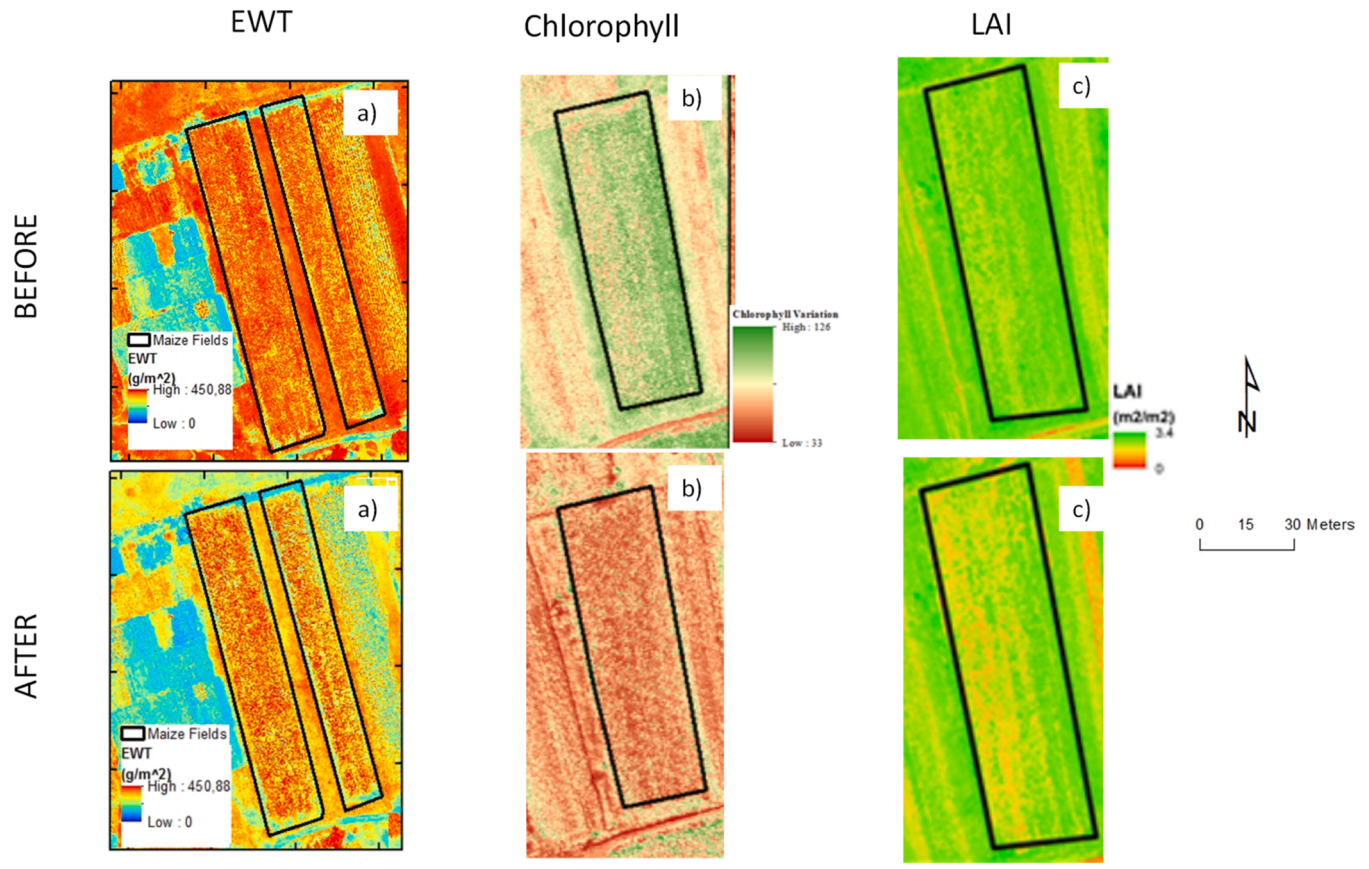

Fig. 7. The spatial distribution of (a) EWT, chlorophyll content, and (c) LAI (i) before and (ii) after the storm based on the optimal spectral features.

contribution of site-specific factors in understanding the effect of natural disasters such as hailstorms on crops.

Conclusion

The main objective of this study was to estimate maize crop health and productivity elements, i.e., EWT, chlorophyll content and LAI, before and after the hailstorm using RPAS remotely sensed data in smallholder croplands as a proxy for gaging the prospects of utilizing RPASs in assessing the effect of hailstorm natural disasters at a field scale. Based on the findings of this study, it can be concluded that the effect of the hailstorm on maize crops

- EWT could be optimally estimated using NDVIrededge, CCCI, CIgreen, NIR and nDVI (NIR/T).
- chlorophyll content variation could be modeled using NDRE, NDWI, Blue NDVIrededge and CCCI, and
- LAI could be estimate using nDVI NIR/T nDVIT/B, nDVI G/R, CIrededge, nDVI B/NIR, GNDVI, BNDVI

The red edge-derived spectral variables had more influence in estimating the effect of the hailstorm on all maize crop's health and productivity elements. These findings underscore the prospects of RPAS-based remote sensing techniques in providing near-real-time spatial information for assessing the impact of hailstorms as natural disasters on the crop productivity in smallholder croplands and its effect on the crops.

Declaration of generative AI and AI-assisted technologies in the writing process

During the preparation of this work the author(s) did not use any AI tools at any stage of the manuscript writing process.

Author contributions

Conceptualization, M.S. and T.N.M.; methodology, K.B., A.C., M.S., J.O; O.M; H.N, S.B; V.G.P.C; and T.M.; software, K.B., A.C., M.S. and T.M.; validation, K.B., M.S. and A.C.; formal analysis, K.B., M.S. and A.C.; investigation, K.B., M.S., A.C., S.G. and T.M.; resources, M.S and T.M.; data curation, K.B.; writing—original draft preparation, K.B; H.N, S.B; and M.S.; writing—review and editing, all authors.; supervision, O.J; T.N.M; A.C. and M.S.; project administration, M.S. and T.M.; funding acquisition, T.M. and M.S. All authors have read and agreed to the published version of the manuscript.

Funding

The WRC, through the centre for Transformative Agricultural and Food Systems (CTAFS) funded this research. Specifically, this research was funded by the Water Research Commission of South Africa (WRC) through Project WRC K5/2971//4 titled "Use of drones in monitoring crop health, water stress, crop water requirements, and improvements on crop water productivity to enhance precision agriculture and irrigation scheduling. Also, we wish to express our gratitude to the Faculty of Arts, University of the Western Cape, for providing funding for the writing retreats that led to the generation of this work.

Declaration of Competing Interest

The authors declare that they have no known competing financial interests or personal relationships that could have appeared to influence the work reported in this paper.

Data availability

Data will be made available on request.

References

[1] E.M. Abdel-Rahman, F.B. Ahmed, R. Ismail, Random forest regression and spectral band selection for estimating sugarcane leaf nitrogen concentration using EO-1 Hyperion hyperspectral data, Int. J. Rem. Sens. 34 (2) (2013) 712–728.

[2] E. Adam, O. Mutanga, D. Rugege, R. Ismail, Discriminating the papyrus vegetation (Cyperus papyrus L.) and its co-existent species using random forest and hyperspectral data resampled to HYMAP, Int. J. Rem. Sens. 33 (2) (2012) 552–569.

[3] T. Adugna, W. Xu, J. Fan, Comparison of random forest and support vector machine classifiers for regional land cover mapping using coarse resolution FY-3C images, Rem. Sens. (Basel) 14 (3) (2022) 574.

[4] E. Barnes, T. Clarke, S. Richards, P. Colaizzi, J. Haberland, M. Kostrzewski, P. Waller, C. Choi, E. Riley, T. Thompson, Coincident detection of crop water stress, nitrogen status and canopy density using ground based multispectral data, in: Proceedings of the fifth international conference on precision agriculture, Bloomington, MN, USA, 2000.

[5] M. Belgiu, L. Dragut, Random forest in remote sensing: a review of applications and future directions, ISPRS J. Photogramm. Rem. Sens. 114 (2016) 24–31.

[6] G.S. Birth, G.R. McVey, Measuring the color of growing turf with a reflectance spectrophotometer 1, Agron. J. 60 (6) (1968) 640–643.

[7] D. Blair, C.M. Shackleton, P.J. Mograbi, Cropland abandonment in South African smallholder communal lands: land cover change (1950–2010) and farmer perceptions of contributing factors, Land (Basel) 7 (4) (2018) 121.

[8] V.K. Boken, C.F. Shaykewich, Improving an operational wheat yield model using phenological phase-based Normalized Difference Vegetation Index, Int. J. Rem. Sens. 23 (20) (2002) 4155–4168.

[9] K. Brewer, A. Clulow, M. Sibanda, S. Gokool, V. Naiken, T. Mabhaudhi, Predicting the chlorophyll content of maize over phenotyping as a proxy for crop health in smallholder farming systems, Rem. Sens. (Basel) 14 (3) (2022) 518.

[10] J. Chang-Hua, T. Yong-Chao, Y. Xia, C. Wei-Xing, Z. Yan, D. Hannaway, Estimating leaf chlorophyll content using red edge parameters, Pedosphere 20 (5) (2010) 633–644.

[11] T. Chapagain, M.N. Raizada, Impacts of natural disasters on smallholder farmers: gaps and recommendations, Agric. Food Secur. 6 (1) (2017) 39.

[12] W. Chivasa, O. Mutanga, C. Biradar, Application of remote sensing in estimating maize grain yield in heterogeneous African agricultural landscapes: a review, Int. J. Rem. Sens. 38 (23) (2017) 6816–6845.

[13] W. Chivasa, O. Mutanga, C. Biradar, UAV-based multispectral phenotyping for disease resistance to accelerate crop improvement under changing climate conditions, Rem. Sens. (Basel) 12 (15) (2020) 2445.

[14] P.J. Curran, J.L. Dungan, H.L. Gholz, Exploring the relationship between reflectance red edge and chlorophyll content in slash pine, Tree Physiol. 7 (1–2–3–4) (1990) 33–48.

[15] M. Dlamini, G. Chirima, M. Sibanda, E. Adam, T. Dube, Characterizing leaf nutrients of wetland plants and agricultural crops with nonparametric approach using sentinel-2 imagery data, Rem. Sens. (Basel) 13 (21) (2021) 4249.

[16] D. Doktor, A. Lausch, D. Spengler, M. Thurner, Extraction of plant physiological status from hyperspectral signatures using machine learning methods, Rem. Sens. (Basel) 6 (12) (2014) 12247–12274.

[17] D.M. El-Shikha, E.M. Barnes, T.R. Clarke, D.J. Hunsaker, J.A. Haberland, P. Pinter Jr, P.M. Waller, T.L. Thompson, Remote sensing of cotton nitrogen status using the canopy chlorophyll content index (CCCI), Trans. ASABE 51 (1) (2008) 73–82.

[18] I. Filella, J. Penuelas, The red edge position and shape as indicators of plant chlorophyll content, biomass and hydric status, Int. J. Rem. Sens. 15 (7) (1994) 1459–1470.

[19] C. Funk, M.E. Budde, Phenologically-tuned MODIS NDVI-based production anomaly estimates for Zimbabwe, Rem. Sens. Environ. 113 (1) (2009) 115–125.

[20] B.-C. Gao, NDWI—A normalized difference water index for remote sensing of vegetation liquid water from space, Rem. Sens. Environ. 58 (3) (1996) 257–266.

[21] D.M. Gates, Leaf temperature and transpiration 1, Agron. J. 56 (3) (1964) 273–277.

[22] A. Gitelson, M.N. Merzlyak, Quantitative estimation of chlorophyll-a using reflectance spectra: experiments with autumn chestnut and maple leaves, J. Photochem. Photobiol. B 22 (3) (1994) 247–252.

[23] A.A. Gitelson, Y. Gritz, M.N. Merzlyak, Relationships between leaf chlorophyll content and spectral reflectance and algorithms for non-destructive chlorophyll assessment in higher plant leaves, J. Plant Physiol. 160 (3) (2003) 271–282.

[24] A.A. Gitelson, M.N. Merzlyak, Remote estimation of chlorophyll content in higher plant leaves, Int. J. Rem. Sens. 18 (12) (1997) 2691–2697.

[25] F. Haghighian, S. Yousefi, S. Keesstra, Identifying tree health using sentinel-2 images: a case study on Tortrix viridana L. infected oak trees in Western Iran, Geocarto Int. 37 (1) (2022) 304–314.

[26] H. Havenga, Characteristics of Hailstorms over the South-African Highveld, North-West University, 2018. http://repository.nwu.ac.za/handle/10394/31246. Assessed 14 August 2023.

[27] A. Huete, K. Didan, T. Miura, E.P. Rodriguez, X. Gao, L.G. Ferreira, Overview of the radiometric and biophysical performance of the MODIS vegetation indices, Rem. Sens. Environ. 83 (1–2) (2002) 195–213.

[28] A.R. Huete, A soil-adjusted vegetation index (SAVI), Rem. Sens. Environ. 25 (3) (1988) 295–309.

[29] E.R. Hunt Jr., B.N. Rock, Detection of changes in leaf water content using near-and middle-infrared reflectances, Rem. Sens. Environ. 30 (1) (1989) 43–54.

[30] Z. Jiang, A.R. Huete, K. Didan, T. Miura, Development of a two-band enhanced vegetation index without a blue band, Rem. Sens. Environ. 112 (10) (2008) 3833–3845.

[31] A. Kamara, A. Conteh, E.R. Rhodes, R.A. Cooke, The relevance of smallholder farming to African agricultural growth and development, Afr. J. Food Agric. Nutr. Dev. 19 (1) (2019) 14043–14065.

[32] E.B. Knipling, Physical and physiological basis for the reflectance of visible and near-infrared radiation from vegetation, Rem. Sens. Environ. 1 (3) (1970) 155–159.

[33] W. Li, C. Liu, Y. Yang, M. Awais, W. Li, P. Ying, W. Ru, M.J.M. Cheema, A UAV-aided prediction system of soil moisture content relying on thermal infrared remote sensing, Int. J. Environ. Sci. Technol. 19 (10) (2022) 9587–9600.

[34] M. Louhaichi, M.M. Borman, D.E. Johnson, Spatially located platform and aerial photography for documentation of grazing impacts on wheat, Geocarto Int 16 (1) (2001) 65–70.

[35] J. Markwell, J.C. Osterman, J.L. Mitchell, Calibration of the Minolta SPAD-502 leaf chlorophyll meter, Photosyn. Res. 46 (3) (1995) 467–472.

[36] T. Miura, H. Yoshioka, K. Fujiwara, H. Yamamoto, Inter-comparison of ASTER and MODIS surface reflectance and vegetation index products for synergistic applications to natural resource monitoring, Sensors 8 (4) (2008) 2480–2499.

[37] O. Mutanga, E. Adam, M.A. Cho, High density biomass estimation for wetland vegetation using WorldView-2 imagery and random forest regression algorithm, Int. J. Appl. Earth Obs. Geoinf. 18 (2012) 399–406.

[38] H. Naito, S. Ogawa, M.O. Valencia, H. Mohri, Y. Urano, F. Hosoi, Y. Shimizu, A. L. Chavez, M. Ishitani, M.G. Selvaraj, Estimating rice yield related traits and quantitative trait loci analysis under different nitrogen treatments using a simple tower-based field phenotyping system with modified single-lens reflex cameras, ISPRS J. Photogramm. Remote Sens. 125 (2017) 50–62.

[39] H. Naito, S. Ogawa, M.O. Valencia, H. Mohri, Y. Urano, F. Hosoi, Y. Shimizu, A. L. Chavez, M. Ishitani, M.G. Selvaraj, K. Omasa, Estimating rice yield related traits and quantitative trait loci analysis under different nitrogen treatments using a simple tower-based field phenotyping system with modified single-lens reflex cameras, ISPRS J. Photogramm. Remote Sens. 125 (2017) 50–62.

[40] H.S. Ndlovu, J. Odindi, M. Sibanda, O. Mutanga, A. Clulow, V.G.P. Chimonyo, T. Mabhaudhi, A comparative estimation of maize leaf water content using machine learning techniques and unmanned aerial vehicle (UAV)-based proximal and remotely sensed data, Rem. Sens. (Basel) 13 (20) (2021) 4091.

[41] A. Ngie, F. Ahmed, K. Abutaleb, Remote sensing potential for investigation of maize production: review of literature, South Afr. J. Geomat. 3 (2) (2014) 163–184.

[42] Z. Qiu, H. Xiang, F. Ma, C. Du, Qualifications of rice growth indicators optimized at different growth stages using unmanned aerial vehicle digital imagery, Rem. Sens. (Basel) 12 (19) (2020) 3228.

[43] A.T. Rädler, P.H. Groenemeijer, E. Faust, R. Sausen, T. Púčik, Frequency of severe thunderstorms across Europe expected to increase in the 21st century due to rising instability, npj Clim. Atmos. Sci. 2 (1) (2019) 30.

[44] V.S. Rana, S. Sharma, N. Rana, U. Sharma, V. Patiyal, Banita, H. Prasad, Management of hailstorms under a changing climate in agriculture: a review, Environ. Chem. Lett. 20 (6) (2022) 3971–3991.

[45] G. Rondeaux, M. Steven, F. Baret, Optimization of soil-adjusted vegetation indices, Rem. Sens. Environ. 55 (2) (1996) 95–107.

[46] J. Rousel, R. Haas, J. Schell, D. Deering, Monitoring vegetation systems in the great plains with ERTS, in: Proceedings of the Third Earth Resources Technology Satellite—1 Symposium; NASA SP-351, NASA, Washington, D.C., 1973.

[47] Rymbai, H., N. Deshmukh, V. Verma, H. Talang and A. Jha (2019). "Impact assessment of hailstorm on khasi mandarin and other horticultural crops in Umiam, Meghalaya".

[48] L.H. Samberg, J.S. Gerber, N. Ramankutty, M. Herrero, P.C. West, Subnational distribution of average farm size and smallholder contributions to global food production, Environ. Res. Lett. 11 (12) (2016), 124010.

[49] H.-D. Seelig, A. Hoehn, L. Stodieck, D. Klaus, W. Adams Iii, W. Emery, Relations of remote sensing leaf water indices to leaf water thickness in cowpea, bean, and sugarbeet plants, Rem. Sens. Environ. 112 (2) (2008) 445–455.

[50] H.D. Seelig, A. Hoehn, L. Stodieck, D. Klaus, W. Adams Iii, W. Emery, The assessment of leaf water content using leaf reflectance ratios in the visible, near-, and short-wave-infrared, Int. J. Rem. Sens. 29 (13) (2008) 3701–3713.

[51] H.M. Shafri, M.M. Salleh, A. Ghiyamat, Hyperspectral remote sensing of vegetation using red edge position techniques, Am. J. Appl. Sci. 3 (6) (2006) 1864–1871.

[52] B. Shiferaw, B.M. Prasanna, J. Hellin, M. Bänziger, Crops that feed the world 6. Past successes and future challenges to the role played by maize in global food security, Food Secur. 3 (3) (2011) 307.

[53] M. Sibanda, O. Mutanga, T. Dube, P.L. Mafongoya, Spectrometric proximally sensed data for estimating chlorophyll content of grasslands treated with complex fertilizer combinations, J. Appl. Rem. Sens. 14 (2) (2020), 024517-024517.

[54] A. Simic Milas, M. Romanko, P. Reil, T. Abeysinghe, A. Marambe, The importance of leaf area index in mapping chlorophyll content of corn under different agricultural treatments using UAV images, Int. J. Rem. Sens. (2018) 1–17.

[55] G.E. Soto, C.G. Pérez-Hernández, I.J. Hahn, A.D. Rodewald, P.M. Vergara, Tree senescence as a direct measure of habitat quality: linking red-edge Vegetation Indices to space use by Magellanic woodpeckers, Rem. Sens. Environ. 193 (2017) 1–10.

[56] M.N. Tahir, S.Z.A. Naqvi, Y. Lan, Y. Zhang, Y. Wang, M. Afzal, M.J.M. Cheema, S. Amir, Real time estimation of chlorophyll content based on vegetation indices derived from multispectral UAV in the kinnow orchard, Int. J. Precis. Agric. Aviat. 1 (1) (2018).
[57] K. Tesfaye, S. Gbegbelegbe, J.E. Cairns, B. Shiferaw, B.M. Prasanna, K. Sonder, K. Boote, D. Makumbi, R. Robertson, Maize systems under climate change in sub-Saharan Africa: potential impacts on production and food security, Int. J. Clim. Change Strat. Manag. (2015).
[58] C.J. Tucker, Red and photographic infrared linear combinations for monitoring vegetation, Rem. Sens. Environ. 8 (2) (1979) 127–150.
[59] M. Vincini, E. Frazzi, P. D'Alessio, A broad-band leaf chlorophyll vegetation index at the canopy scale, Precis. Agric. 9 (2008) 303–319.
[60] I. Wahab, O. Hall, M. Jirström, Remote sensing of yields: application of uav imagery-derived ndvi for estimating maize vigor and yields in complex farming systems in Sub-Saharan Africa, Drones 2 (3) (2018) 28.
[61] F.-M. Wang, J.-f. HUANG, Y.-l. TANG, X.-z. WANG, New vegetation index and its application in estimating leaf area index of rice, Rice Sci. 14 (3) (2007) 195–203.
[62] C. Wu, Z. Niu, Q. Tang, W. Huang, Estimating chlorophyll content from hyperspectral vegetation indices: modeling and validation, Agric. For. Meteorol. 148 (8–9) (2008) 1230–1241.
[63] F.-f. YANG, L. Tao, Q.-y. WANG, M.-z. DU, T.-l. YANG, D.-z. LIU, S.-j. LI, S.-p. LIU, Rapid determination of leaf water content for monitoring waterlogging in winter wheat based on hyperspectral parameters, J. Integr. Agric. 20 (10) (2021) 2613–2626.
[64] S.A.D.M. Zahir, A.F. Omar, M.F. Jamlos, M.A.M. Azmi, J. Muncan, A review of visible and near-infrared (Vis-NIR) spectroscopy application in plant stress detection, Sens. Actuat., A (2022), 113468.
[65] F. Zhang, G. Zhou, Estimation of vegetation water content using hyperspectral vegetation indices: a comparison of crop water indicators in response to water stress treatments for summer maize, BMC Ecol. 19 (1) (2019) 18.
[66] L. Zhang, H. Zhang, Y. Niu, W. Han, Mapping maize water stress based on UAV multispectral remote sensing, Rem. Sens. (Basel) 11 (6) (2019) 605.